

Supplemental Information

Weathering of a Carbon Nanotube/Epoxy Nanocomposite under UV Light and in Water Bath: Impact on Abraded Particles

Lukas Schlagenhauf, Bahareh Kianfar, Tina Buerki-Thurnherr, Yu-Ying Kuo,
Adrian Wichser, Frank Nüesch, Peter Wick, and Jing Wang

1 Properties of the used multi-wall carbon nanotubes (MWCNTs)

Table S.1. Properties of Baytubes C150p by Bayer Material Science (Bayer Material Science, 2012 [1], Thurnherr et al. 2009 [2], Schlagenhauf et al. 2015 [3], Wang et al. 2015 [4])

Property	Manufacturer's specification		Authors' characterization	
	Value	Method	Value	Method
C-Purity	> 95 %	Elemental analysis		
Free amorphous carbon	Not detectable	TEM	Not detectable	TEM
Impurities			Co (0.2 ~ 0.4 wt%), Mn (~ 0.3 wt%), Mg (0.4 wt%) and Ni (0.006 wt%)	ICP-OES
Number of walls	3 – 15	TEM		
Outer mean diameter	13 – 16 nm	TEM		
Outer diameter distribution	5 – 20 nm	TEM	6 – 20 nm	TEM
Inner mean diameter	4 nm	TEM		
Inner diameter distribution	2 – 6 nm	TEM	1 – 10 nm	TEM
Length	1 – >10 μm	SEM	2 – 4 μm	SEM
Bulk density	0.14 – 0.16 g/cm^3	EN ISO 60		
Intrinsic density of the graphite layers			2.19 g/cm^3	Pycnometry and mass
Agglomeration status			Highly entangled	SEM

2 Water uptake

Table S.2: Comparison of different water uptake studies for CNT/epoxy nanocomposites with the obtained results in this study, shown are the effects of the addition of CNTs on the equilibrium water uptake M_∞ and the diffusion coefficient D_T

Study	CNT content	M_∞	D_T
Barkoula <i>et al.</i> [5]	0.3 – 1 wt%	↑	↑
Guadagno <i>et al.</i> [6]	0.5 – 2 wt%	↓	↓
Prolongo <i>et al.</i> [7]	0.1 – 0.25 wt%	↓	↓
Starkova <i>et al.</i> [8]	0.3 – 1 wt%	—	↓
This study	0.1 – 1 wt%	↑	↑

3 Additional information on the ATR-FTIR measurements

Table S.3: Identified peaks on the ATR-FTIR graphs

Peak (cm⁻¹)	Excitation
3700 – 3100	OH and NH stretching vibration
1740	C=O stretching vibration
1650	C=O stretching vibration
1608	C=C stretching vibration
1581	C=C stretching vibration
1510	C=C stretching vibration
1460	CH ₃ - and CH ₂ - deformation, CH ₂ -O deformation
1370 – 1390	CH ₃ symmetric deformation
1295	C-N stretch aromatic amine, C-C stretching, vibration aromatic ring
1245	C-O-C aromatic ether stretching deformation, bridge between benzene rings
1180	C-C symmetrical stretching vibration
1100	C-O-C out of plane deformation in aromatic rings, C-N symmetrical stretching vibration
1037	C-O symmetrical stretching
930	Antisymmetric deformation of epoxy ring
827	Aromatic C-H out of plane deformation

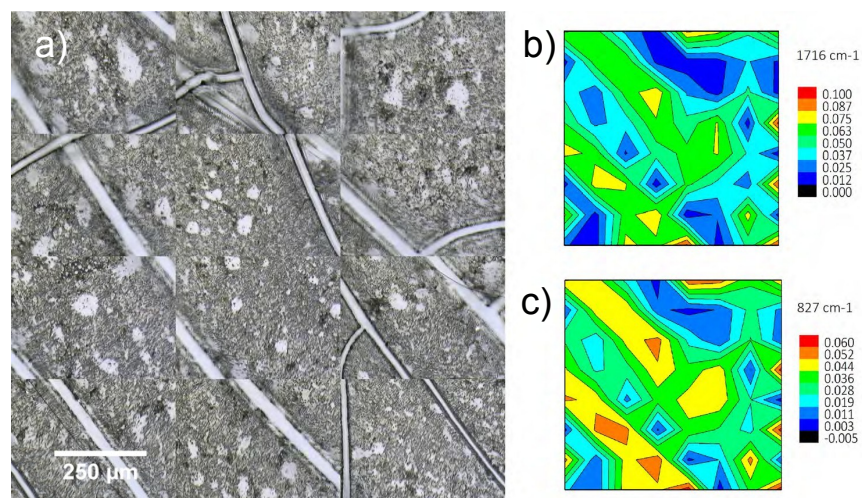


Figure S.1: a) Light microscopy raster image of a 1 wt% CNT/epoxy sample, exposed to UV light for 1500 h. Right: Contour plots of the absorbance of b) the 1716 cm^{-1} peak and c) the 827 cm^{-1} peak.

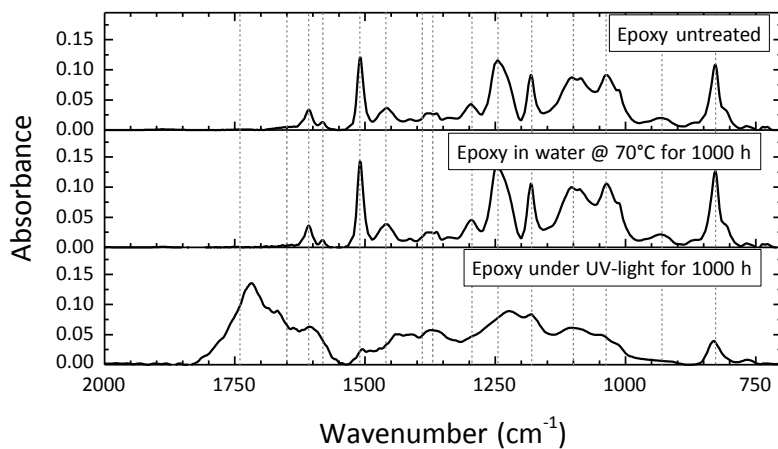


Figure S.2: ATF-FTIR measurements of the epoxy weathering samples after 1000 h compared to untreated epoxy. The vertical lines indicate the identified peaks given in Tab. S.3

4 Surface chemistry after weathering at elevated temperatures

Both presented weathering processes in the main manuscript were conducted at elevated temperatures. To identify temperature effects on the surface chemistry, also weathering at elevated temperatures, low RH, and no light was carried out in a furnace under ambient air for 1000 h. The temperature was set to 70 °C and the measured RH was below 5 %. The ATR-FTIR measurement in Figure. S.3 shows that compared to the unaffected water bath sample that also was exposed to 70 °C for 1000 h, two new peaks were formed at 1735 cm^{-1} and at 1650 cm^{-1} .

Those two peaks can be attributed to a C=O formation, caused either by chain scission or by oxidation of the polymer. It can be assumed, that the peaks are caused by oxidation, because for the water bath samples at the same temperature, but with a limited presence of oxygen, no such effect appears. The growth of the two additional peaks can be fitted by usage of the peak at 1508 cm^{-1} as reference. The result is shown in Figure. S.4. The growth seems to be linear and no difference between the neat epoxy and the nanocomposites can be recognized.

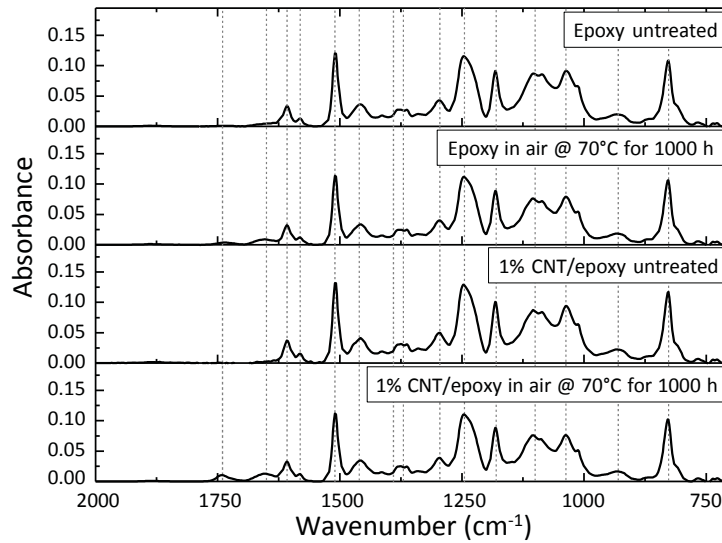


Figure S.3: ATF-FTIR measurements of the neat epoxy and the 1 wt% CNT/epoxy composite for weathering at 70 °C for 1000 h compared to untreated samples. The vertical lines indicate the identified peaks in Tab. S.3

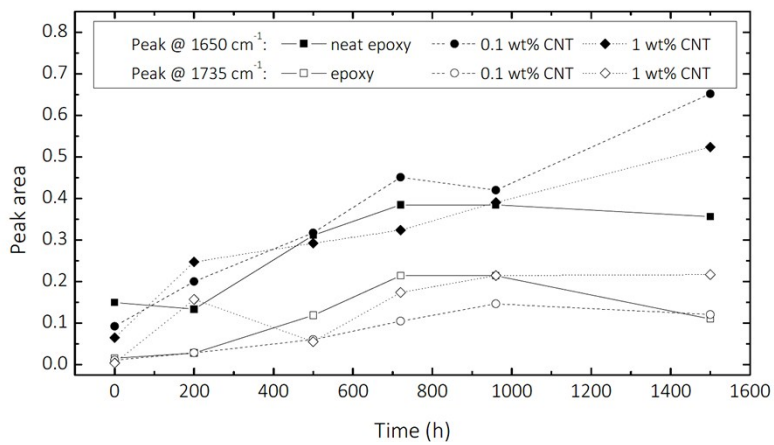


Figure S.4: Areas of the peaks at 1735cm⁻¹ and at 1650cm⁻¹ during the heat treatment at 70 °C for three samples, a neat epoxy and two nanocomposites with 0.1 wt% and 1 wt% of CNTs. The lines are inserted to guide the eye.

5 Modes of the measured particle size distributions

Table S.4: The values of the peak maxima, given in μm , from the obtained size distributions of the abrasion experiments. For mode 1, detected by SMPS, no change between the start and the end of the experiment was measured. For the modes 2 & 3, measured by APS, the start and end values are reported.

Sample	Treatment	Mode 1	Mode 2 surface	Mode 2 bulk	Mode 3 surface	Mode 3 bulk
Neat epoxy	Untreated	0.384	0.721	0.708	1.466	1.186
	1000 h water bath at 70 °C	0.374	0.991	0.676	2.407	1.281
	500 h under UV light	0.358	0.772	0.661	1.642	1.268
	1000 h under UV light	0.383	1.120	0.712	2.694	1.650
	1500 h under UV light	0.415	0.724	0.677	1.705	1.395
1 wt% CNT	Untreated	0.375	1.043	0.666	2.250	1.078
	1000 h water bath at 70 °C	0.367	1.090	0.657	2.403	1.176
	500 h under UV light	0.371	0.847	0.689	2.190	1.522
	1000 h under UV light	0.397	1.035	0.699	2.476	1.572
	1500 h under UV light	0.406	0.760	0.686	1.589	1.285

References

1. Bayer Material Science (2012). Product Information Baytubes C150p. Retrieved from http://www.baytubes.com/product_production/baytubes_data.html.
2. T. Thurnherr, D. S. Su, L. Diener, G. Weinberg, P. Manser, N. Pfänder, R. Arrigo, M. E. Schuster, P. Wick, H. F. Krug, N. Pfander, R. Arrigo, M. E. Schuster, P. Wick, H. F. Krug. Comprehensive evaluation of in vitro toxicity of three large-scale produced carbon nanotubes on human Jurkat T cells and a comparison to crocidolite asbestos. *Nanotoxicology*, 3(4): 319–338, 2009.
3. R. Hollertz, S. Chatterjee, H. Gutmann, T. Geiger, F. A. Nueesch, B. T. T. Chu. Improvement of toughness and electrical properties of epoxy composites with carbon nanotubes prepared by industrially relevant processes. *Nanotechnology*, 22:125702, 2011.
4. J. Wang, Y. K. Bahk, S.-C. Chen, D. Y. H. Pui. Characteristics of airborne fractal-like agglomerates of carbon nanotubes, *Carbon*, 93:441–450, 2015.
5. N. M. Barkoula, A. Paipetis, T. Matikas, A. Vavouliotis, P. Karapappas, and V. Kostopoulos. Environmental degradation of carbon nanotube-modified composite laminates: a study of electrical resistivity. *Mechanics of Composite Materials*, 45(1):21–32, 2009.
6. L. Guadagno, L. Vertuccio, A. Sorrentino, M. Raimondo, C. Nadeo, V. Vittoria, G. Iannuzzo, E. Calvi, S. Russo. Mechanical and barrier properties of epoxy resin filled with multi-walled carbon nanotubes. *Carbon*, 47(10):2419–2430, 2009.
7. S. G. G Prolongo, M. R. R Gude, A. Ureña. Water uptake of epoxy composites reinforced with carbon nanofillers. *Composites Part A: Applied Science and Manufacturing*, 43(12):2169–2175, 2012.
8. O. Starkova, S. T. Buschhorn, E. Mannov, K. Schulte, A. Aniskevich. Water transport in

epoxy/MWCNT composites. *European Polymer Journal*, 49(8):2138–2148, 2013.